

Probing the sign of on-site Hubbard interaction by two-particle quantum walks

Andrea Beggi, Luca Razzoli, Paolo Bordone*

*Dipartimento di Scienze Fisiche, Informatiche e Matematiche,
Università di Modena e Reggio Emilia, I-41125, Modena, Italy and
Centro S3, CNR-Istituto di Nanoscienze, I-41125, Modena, Italy*

Matteo G. A. Paris†

Quantum Technology Lab, Dipartimento di Fisica dell'Università degli Studi di Milano, I-20133 Milano, Italy

(Dated: July 30, 2018)

We consider two identical bosons propagating on a one-dimensional lattice and address the problem of discriminating whether their mutual on-site interaction is attractive or repulsive. We suggest a probing scheme based on the properties of the corresponding two-particle quantum walks, and show that the sign of the interaction introduces specific and detectable features in the dynamics of quantum correlations, thus permitting to discriminate between the two cases. We also discuss how these features are connected to the band-structure of the Hubbard Hamiltonian, and prove that discrimination may be obtained only when the two walkers are initially prepared in a superposition of localized states.

I. INTRODUCTION

The Hubbard model (HM) [1–3] describes the physics of several systems of correlated bosons (or fermions) [4] on different platforms, e.g. ultracold atomic lattices [5–8], spin chains [9, 10] and nonlinear waveguides [11–15]. The same model [9, 16] may be also employed to describe the propagation of identical (and interacting) particles [17–19] on a one-dimensional lattice. In these systems, the on-site interaction can be either attractive or repulsive, depending on the chosen physical implementation. Remarkably, there are systems where both possibilities are contemplated [12, 20–22].

Recent experimental results with cold atoms have shown that a bounded pair of interacting particles may be formed even under the action of a repulsive potential [5, 21, 23–25]. This phenomenon may be understood by looking at the band-structure of the model, which behaves symmetrically under the exchange of sign in the interaction term: in both cases the onset of the interaction creates a separate *mini-band* hosting bounded states, thus determining the co-propagation of the particles that are initially placed on the same site [11, 26]. This feature has suggested the hypothesis that the model is fully symmetrical under the exchange of sign of the on-site interaction, and this conjecture was somehow corroborated by the fact that no differences may be seen in the correlations among particles [11], at least when localized initial states are considered.

At variance with these results, more recent studies on the Hubbard dynamics of identical particles [14, 27, 28] have shown that depending on the nature of the initial states, the HM may indeed lead to different dynamics if we switch the sign of the on-site interaction. Besides the

fundamental interest, this fact may be useful to engineer entanglement at a deeper level, thus granting a further degree of freedom to perform (quantum) computational tasks.

Following the considerations above, here we address the discrimination between attractive and repulsive on-site interaction in the Hubbard model. In particular, we analyze the dynamics of two identical bosons propagating on a one-dimensional lattice and show that the sign of the interaction clearly influences the evolution of the system, as well as the nature of the particle correlations, thus permitting the discrimination between the two cases. We also devote attention to prove that i) these features are intimately connected to the band-structure of the Hubbard Hamiltonian and ii) discrimination is possible when the two particles are initially prepared in a *superposition* of localized states, whereas for localised states no differences may be observed [11, 26].

Our probing scheme is based on the fact that the Hubbard Hamiltonian describes the quantum walks of identical particles on a one-dimensional lattice. In turn, we consider the two identical bosons as quantum probes [29–32] and the dynamical feature of their quantum walks as a tool to reveal the sign of the interaction. Besides, we will also develop an intuitive picture for their behaviour, adding on previous observations [27].

Quantum walks (QWs) describe the dynamics of one or more quantum particles on a lattice [33, 34]. They show characteristic quantum features when compared to their classical counterparts, e.g. ballistic propagation, coherent superposition and interference. These effects make QWs suitable for the implementation of quantum algorithms [35–38]. In turn, those potential applications inspired a series of experiments, especially with optical networks [39–42], see [43] for a more comprehensive review. In particular, experimental realizations of photonic quantum walks [40, 44–46], have provided suitable architectures that outperform their classical counterparts for some specific tasks. In these systems, QWs are typically

*Electronic address: paolo.bordone@unimore.it

†Electronic address: matteo.paris@fisica.unimi.it

performed by identical particles and indistinguishability of the walkers may, in turn, build up genuinely quantum correlations even in the absence of interaction between the particles [47, 48], as it was observed experimentally in photonic waveguides [39, 40, 49].

In order to characterize the sign of the on-site interaction we analyze in details the dynamics of the two walkers and the time evolution of their quantum correlations with focus on entanglement. In turn, despite entanglement among identical particles has raised much interest [50–68], no universally accepted measure for its quantification is present. On the other hand, among the different criteria, the so-called *entanglement of particles* [58] is perhaps the most convenient, due to its simple computability, and to the fact that it may be accessible in practical scenarios [59]. Indeed, it has been recently employed to quantify quantum correlations in spin chains [69, 70], where it also detects quantum phase transitions, and in model systems of QWs described by the Hubbard Hamiltonian [28, 48, 71].

The paper is organized as follows: in Section II we introduce the bosonic Hubbard-model, whereas in Section III we briefly review the theoretical tools to quantify entanglement between the walkers. In Section IV we illustrate the behaviour of the two walkers by numerically solving the dynamics for a chain with $N = 30$ sites, whereas in Section V we discuss the results with the help of a simplified semi-analytical model (a reduced chain with $N = 4$ sites). Finally, Section VI closes the paper with some concluding remarks, and Appendix A presents some further discussions about the symmetries of the system, in order to better appreciate the results presented in the body of the paper.

II. THE INTERACTION MODEL AND THE BAND-STRUCTURE

The Bose-Hubbard Hamiltonian describes a collection of spinless bosons propagating on a one-dimensional made of N sites, with periodic boundary conditions ($N + 1 = 1$). The Hamiltonian ($\hbar = 1$), it is given by:

$$H_N(J, V) = -Jh_N(v) \quad (1)$$

$$h_N(v) = -\sum_{i=1}^N c_{i+1}^\dagger c_i + c_i^\dagger c_{i+1} + \frac{v}{2} \sum_{i=1}^N n_i(n_i - 1)$$

where c_i (c_i^\dagger) is the operator that destroys (creates) a particle on site i of the chain, J is the hopping amplitude, V is the strength of the interaction among the bosons sharing the same site (attractive for $V < 0$, repulsive for $V > 0$) and $v = V/J$ is the relative strength of the interaction with respect to the hopping energy. In the following we focus on a system with total number of particles $n = 2$. Since J is only a time-dilation factor, giving the characteristic time of the hopping dynamics, we introduce the dimensionless time $\tau = |J|t$. The quantity v

is thus the sole parameter influencing the physics of the system.

The states of the system can be equally represented in the Fock space and in the symmetrized two-particle Hilbert space, with dimension $N(N + 1)/2$ and basis set given by $\{|1, 1\rangle_s, |1, 2\rangle_s, \dots, |2, 2\rangle_s, \dots, |N, N\rangle_s\}$, where $|i, j\rangle_s$ ($j \geq i$) stands for a symmetrized state in which one particle is localized on site i , and the other on site j [72]. Since the Hubbard Hamiltonian represents the discrete version of the kinetic operator plus a central potential (depending only on the relative distance among the particles), the dynamics can be factorized in the coordinate space of the center of mass $R = \frac{i+j}{2}$ and the relative distance $r = j - i$, so the ansatz for its eigenfunctions becomes

$$\Phi(R, r) = e^{iKR} \varphi(r), \quad (2)$$

and the energy spectrum $E(K) = \omega(K)$ depends on the quasimomentum K , which assumes only discrete values due to the periodic boundary conditions ($K = \frac{2\pi}{N}\nu$, where $\nu = 1, 2, \dots, N$). The bandstructure [73] is composed by a *mini-band*, hosting N states with energies near V , and a *main subband*, extended approximately between $-4J$ and $+4J$ and hosting the remaining $N(N - 1)/2$ states [11, 26]. The eigenstates in the mini-band are associated with the so-called *bound states*, in which the particles share the same site and show a co-walking dynamics. Conversely, the eigenstates of the main subband, the so-called *scattering states*, have a delocalized wavefunction (with $\varphi(0) \sim 0$) and show a fermionic anti-bunching behaviour in the high V regime [11]. The striking aspect is that also a repulsive potential may create a bound pair of bosons, as it has been shown experimentally [21]. Indeed, the evolution of particles which are initialized in a bound state is dominated by the states of the miniband, which in the high V regime are well separated in energy from the states of the main subband: therefore, the bound-state particles are forced to remain on the same site while performing their quantum walk.

It has been observed [11, 26, 74] that the energy spectrum $\text{Spec}[H_N(J, V)]$ simply changes its sign when we change the sign of V , i.e. $\text{Spec}[H_N(J, V)] = -\text{Spec}[H_N(J, -V)]$ (we consider inverse ordering for the two spectra) and for this reason, it was suggested that the dynamics of the system are the same irrespective of the sign of V [11, 21]. However, this symmetry holds only for chains with even N , whereas for chains with odd N , as it is shown in the left panel of Fig. 1 for $N = 5$, the two spectra display some clear discrepancies (mostly in the main subband). If we refer to the two spectra as $\text{Spec}[H_N(J, \pm V)] = \{\omega_i^\pm\}_i$, we may define the deviation D_V between them as:

$$D_V(N) = \|\text{Spec}[H_N(V)] + \text{Spec}[H_N(-V)]\|$$

$$= \sqrt{\sum_i (\omega_i^+ + \omega_i^-)^2}. \quad (3)$$

The behavior of D_V against N is reported in the right panel of Fig. 1: D_V is always zero for even N , while for odd N it vanishes only in the limit for $N \rightarrow \infty$. This suggests that the considered effect is related to differences in periodic boundary conditions, which are less important as soon as N grows. Our observations on the effects of $\text{sgn}(V)$ over dynamics do not depend on N being even or odd. However, in order to avoid the influence of the asymmetry of the bandstructure, we considered in our simulations only chains with even N . Even in this condition, however, it will be apparent that there are differences in the dynamics when switching from attractive to repulsive interactions (or vice versa).

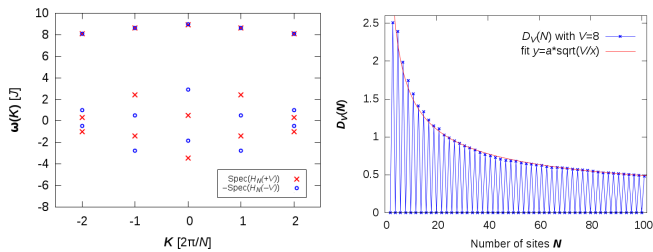


FIG. 1: (Left): band-structure (spectrum) of $H_N(V)$ and $-H_N(-V)$ for $V = 8$ and $N = 5$. Energies are given in units of J , wave-vectors in units of $2\pi/N$. (Right): Deviation $D_V(N)$ between the spectra of $H_N(V)$ and $H_N(-V)$ for $V = 8$ at different values of N . The two spectra are exactly opposite ($D_V(N) = 0$) only for even N . The red line is a phenomenological fit for odd N values.

III. TWO-SITE CORRELATIONS AND ENTANGLEMENT OF PARTICLES

The particle density at each site i of the lattice and the two-particle correlation among sites i and j at a given time t are given by

$$n_i(t) = \langle c_i^\dagger c_i \rangle, \quad (4)$$

$$\Gamma_{i,j}(t) = \langle c_i^\dagger c_j^\dagger c_j c_i \rangle. \quad (5)$$

$\Gamma_{i,j}$ coincides with the diagonal element of the density operator $\rho_{i,j;i,j} = {}_s\langle i, j | \rho | i, j \rangle_s$ whereas for n_i we have $n_i = \sum_i \rho_{i,j;i,j} (1 + \delta_{i,j})$. The two-particle correlation is useful to identify behaviours like bunching (or co-walking) and anti-bunching, which depend both on the initial state $|\Psi(0)\rangle$ and on the strength of the interaction V [11, 17]. Here, we will show that it depends on $\text{sgn}(V)$ for some initial states. In particular, for the sake of simplicity we consider the normalized two-particle correlations:

$$\tilde{\Gamma}_{i,j}(t) = \frac{\Gamma_{i,j}(t)}{\max_{\{i,j\}}[\Gamma_{i,j}(t)]}. \quad (6)$$

In order to quantify the entanglement among the walkers, we employ the *entanglement of particles* E_P [58], i.e.

$$E_P = \sum_{k=0}^n P_{k,n-k} E(\rho_{k,n-k}), \quad (7)$$

where, given a bipartition of the sites $A = \{n_{Ai}\}_i$ and $B = \{n_{Bi}\}_i$

$$\rho_{k,n-k} = \Pi_{k,n-k} \rho \Pi_{k,n-k} \quad (8)$$

is the projection of the system state ρ over the subspace in which A contains exactly k particles and B the remaining $n - k$ ones, whereas $P_{k,n-k} = \text{Tr}[\rho_{k,n-k}]$ is the corresponding probability. For any given bipartition the projectors $\Pi_{k,n-k}$ may be expressed as

$$\Pi_{k,n-k} = \sum_{\Sigma_i n_{Ai}=k} |\{n_{Ai}\}\rangle \langle \{n_{Ai}\}| \otimes \sum_{\Sigma_i n_{Bi}=n-k} |\{n_{Bi}\}\rangle \langle \{n_{Bi}\}|,$$

and satisfy the completeness relation gives $\sum_{k=0}^n \Pi_{k,n-k} = \mathbb{I}$. The quantity E can be any standard measure of bipartite entanglement among the registers individuated by the two partitions. For a two-particle system, the terms with $k = 0$ or $k = 2$ give zero correlations $E = 0$ and thus Eq. (7) reduces to

$$E_P = P_{1,1} E(\rho_{1,1}). \quad (9)$$

Since we are considering a Hamiltonian system, the states remain pure during all their evolution, and we can thus use for the *linear entropy* [53] for E

$$E(\rho_{AB}) = \frac{N}{N-2} (1 - \text{Tr}_A[\rho_A^2]), \quad (10)$$

where $\rho_A = \text{Tr}_B[\rho_{AB}]$ is the reduced density matrix of the subsystem A . Equivalent results may be obtained upon employing the von Neumann entropy or the negativity [75, 76].

It is worth noting that E_P depends upon the chosen bipartition of the system modes among Alice and Bob: therefore, different partitions of the system can lead to different values of E_P . Also, it should be mentioned that E_P does not capture all the quantum correlations encoded in the system: indeed, “ideal” co-walking situations, where the particles are strongly correlated, do not give contributions to E_P (since they correspond to $k = 0$ or $k = 2$). On the other hand, those states cannot be exploited to perform any task, since one of the two observers is left with no particle on which she can perform any local operation. E_P thus appears to capture the presence of quantum correlations that represent a resource for quantum information processing.

IV. PROBING THE SIGN BY TWO-PARTICLE QUANTUM WALKS

In this section we describe how the sign of the interaction may be revealed by the features of the walkers’

dynamics and by their correlations. As a representative situation, we choose a lattice with $N = 30$ sites. The dynamics of the system is driven either by the Hamiltonian $H_+ = H_N(J, V)$ or $H_- = H_N(J, -V)$, where $J = 1$. Their spectra $\omega(K)$ (which are symmetrical with respect to $\omega = 0$) are reported in Fig. 2. In studying the dynamics, we limit ourselves to interaction times such that the two particles remain far from the boundaries of the lattice, in order to avoid interference effects due to periodic boundary conditions. Given the initial preparation $\rho(0) = |\Psi(0)\rangle\langle\Psi(0)|$ of the two particles we evaluate the evolved state $\rho(t) = U_{\pm}(t)\rho(0)U_{\pm}^{\dagger}(t)$, $U_{\pm}(t) = \exp(-iH_{\pm}t)$ by numerical diagonalization of the Hamiltonian(s) [77].

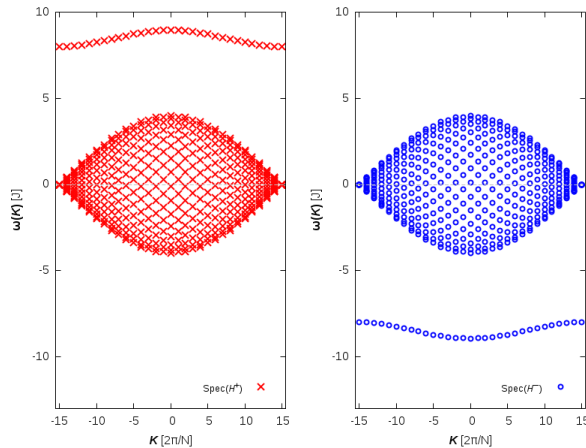


FIG. 2: Bandstructure $\omega(K)$ of a chain with $N = 30$ sites at $V/J = +8$ (left, red) and $V/J = -8$ (right, blue).

As possible initial states $|\Psi(0)\rangle$ we consider the following ones:

$$|\Psi_1\rangle = |15, 17\rangle_s, \quad (11)$$

$$|\Psi_2\rangle = |14, 16\rangle_s, \quad (12)$$

$$|\Psi_3\rangle = |14, 17\rangle_s, \quad (13)$$

$$|\Psi_4\rangle = |14, 16\rangle_s + |15, 17\rangle_s, \quad (14)$$

$$|\Psi_5\rangle = |14, 16\rangle_s + |14, 17\rangle_s, \quad (15)$$

which we evolve, alternatively, under the action of $U_{\pm}(t)$.

Let us start by looking at the behaviour of the correlations $\tilde{\Gamma}_{i,j}$. As it can be seen in the upper panel of Fig. 3, $\tilde{\Gamma}_{i,j}$ for the states $|\Psi_1\rangle$, $|\Psi_2\rangle$ and $|\Psi_3\rangle$ is invariant under the sign exchange of V . The evolution corresponds to the choice $V = \pm 8$, simulations with different values of V lead to the same behavior. Notice that the evolutions of $|\Psi_1\rangle$ and $|\Psi_2\rangle$ are practically identical, except for a rigid shift, and this makes sense since H_N with periodic boundary conditions commutes with the translation operator $T_l = \sum_i |i+l\rangle\langle i|$, therefore two states that differ only for a rigid shift of $l = 1$ sites ($|\Psi_1\rangle = T_1|\Psi_2\rangle$) should have the same dynamics. The same behaviour is found for the entanglement of particles E_P , which is identical both for H_+ and H_- and is reported in the upper

panels of Fig. 4; E_P is initially zero since all states are symmetrized versions of factorizable states. Notice that those initial states are eigenstates of the number operators n_i , i.e. they have an exact number of particles in each site of the lattice. The evolution of these states is invariant when switching from H_+ to H_- [11]. However, the same consideration does not hold, in general, for superpositions of these states [14, 27]: as it can be seen in the lower panel of Fig. 3, the evolution of correlations $\tilde{\Gamma}_{i,j}$ in $|\Psi_4\rangle$ is the same for V and $-V$, whereas the evolution of correlations in $|\Psi_5\rangle$ is appreciably different for attractive and repulsive interactions.

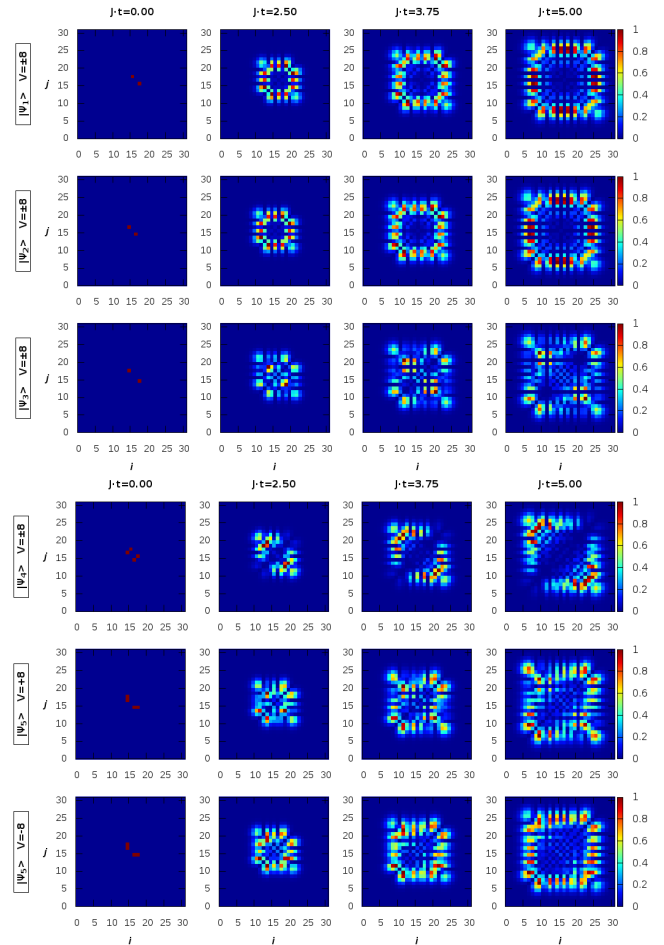


FIG. 3: (Upper panel): Evolution of two-sites correlations $\tilde{\Gamma}_{i,j}$ in states $|\Psi_1\rangle$, $|\Psi_2\rangle$ and $|\Psi_3\rangle$ under H_+ and H_- , with $V = \pm 8$ and $J = 1$. (Lower panel): the same for states $|\Psi_4\rangle$ and $|\Psi_5\rangle$.

The effects of the interaction sign may be seen also in the dynamics of entanglement of particles (see the upper panels of Fig. 4): E_P for $|\Psi_4\rangle$ is independent from the sign of V , while the entanglement of $|\Psi_5\rangle$ is different for V and $-V$ (notice that $E_P(|\Psi_5\rangle)$ is initially 0 since the state is factorizable). Further analysis show that this effect depends on the modulus of $|V|$: in Fig. 5, we see that differences in $\tilde{\Gamma}_{i,j}$ for $|\Psi_5\rangle$ are slightly more marked

at $V = \pm 2$ than at $V = \pm 20$, and the same behaviour is found for entanglement. Indeed, for some states, e.g.

$$|\Psi_6\rangle = |14, 14\rangle_s + |14, 17\rangle_s, \quad (16)$$

at low interaction energy $V/J = \pm 2$, E_P may differ by factor 2, whereas the difference is significantly reduced at higher V (see lower panels of Fig. 4). For this particular state, also the differences in correlations $\tilde{\Gamma}_{i,j}$ (here not reported) are more striking at a lower interaction energy (they are 10 times larger at $V = \pm 2$ compared to what may be seen at $V = \pm 20$).

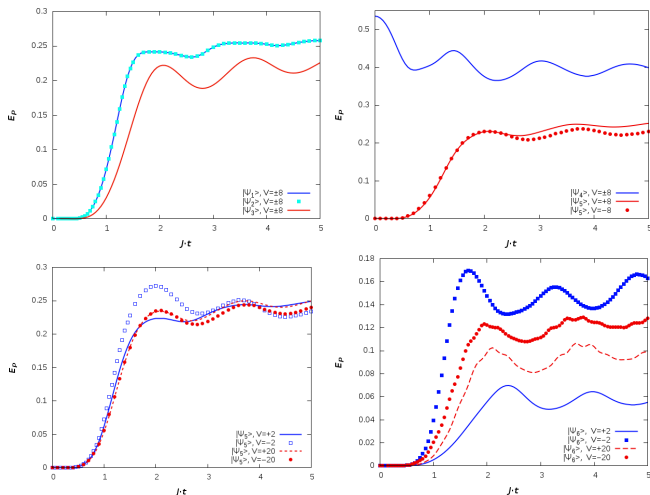


FIG. 4: Time evolution of entanglement of particles under H_{\pm} . (Upper left): states $|\Psi_1\rangle, |\Psi_2\rangle$, $V = \pm 8$. (Upper Right): states $|\Psi_5\rangle$ under H_{\pm} , $V = \pm 8$. (Lower left): state $|\Psi_5\rangle$ and different values of V . (Lower right): state $|\Psi_6\rangle$ and different values of V .

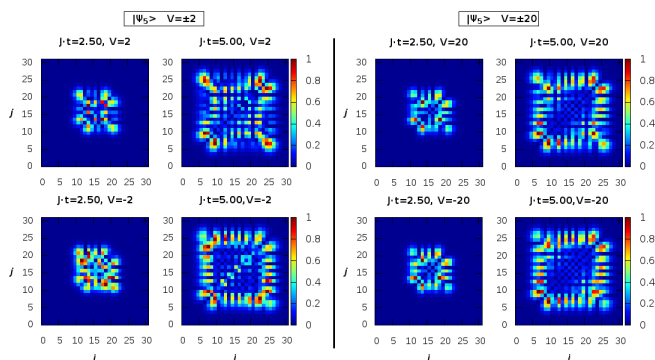


FIG. 5: Evolution of two-sites correlations $\tilde{\Gamma}_{i,j}$ in state $|\Psi_5\rangle$ under H_+ and H_- for different values of V and for $J = 1$. Differences between evolutions are more apparent at low potential energies (i.e. $V \sim J$)

V. A DISCUSSION BASED ON AN ANALYTIC TOY-MODEL WITH FEW SITES

In order to better understand the behaviour of the system, and build an intuitive picture, let us consider an analytic toy-model with a chain made of $N = 4$ sites. In the left panel of Fig. 6 we show the band-structure of $H_{\pm} = H_4(J, \pm V)$ with $J = 1$ and $V = 8$, whereas the behaviour of the eigenvalues of H_+ as a function of V is shown in the central panel. The eigenvalues of H_+ are denoted by ω_i^+ and are reported in Fig. 7, while the eigenvalues of H_- can be obtained by replacing $\omega_i^- = -\omega_i^+$. However, since the system is invariant under time-reversal, any change in the dynamics cannot be related to the simple sign switching of the eigenvalues. The radial part of the eigenfunctions, see Eq. (2), changes sign in some components when switching from H_+ to H_- [26], while others remain unchanged, suggesting that the different behaviours with attractive/repulsive interactions depend on this feature of the eigenstates.

For what concerns the number eigenstates, due to the translational invariance of the chain, the only states which are physically different are $|1, 1\rangle_s$, $|1, 2\rangle_s$ and $|1, 3\rangle_s$. Each of these states can be decomposed by projection on the eigenstates of the Hamiltonian, leading to

$$|j, k\rangle_s = \sum_i C_{j,k,i}^{\pm} |\Phi_i^{\pm}\rangle. \quad (17)$$

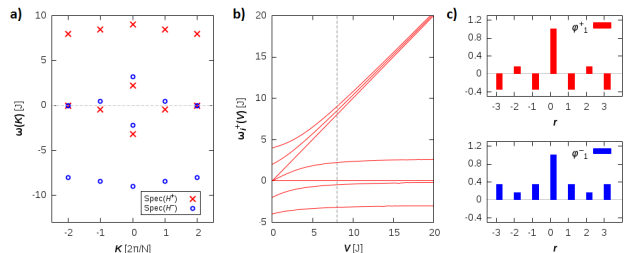


FIG. 6: **a)** Bandstructures for H_+ (red crosses) and H_- (blue dots) at $V = \pm 8$. The main subband and the miniband are clearly visible, as well as the symmetry of the two spectra. **b)** Evolution of the eigenvalues ω_i^+ at increasing V : for high values of the potential energy, there is a clear separation between the miniband (which becomes almost flat) and the main subband, while at low V the two subbands are entwined. The grey vertical dashed line indicates $V = 8$ (subfig. a). **c)** Radial wavefunction for the first eigenstate of H_+ (upper, red) and H_- (lower, blue).

Since the Hamiltonian H_{\pm} are real, it is always possible to choose a set of eigenstates $|\Phi_i^{\pm}\rangle$ having real components in the number states basis, therefore the scalar products

$$C_{j,k,i}^{\pm} = \langle \Phi_i^{\pm} | j, k \rangle_s \quad (18)$$

that we obtain with the projection are real numbers too.

As you can see in Figure 8, all the projections of states like $|1, 1\rangle_s$ and $|1, 3\rangle_s$ do not change sign when we switch

	Eigenvalue	Degen.	
Miniband	ω_1^+	$\frac{V}{3} + \frac{48J^2+V^2}{9\gamma} + \gamma$	1
	$\omega_{2,3}^+$	$\frac{V+\sqrt{16J^2+V^2}}{2}$	2
	ω_4^+	V	1
Main subband	ω_5^+	$V + \omega_1^+(J, -V) - \omega_1^+(J, V) = \frac{V}{3} + \left(\frac{48J^2+V^2}{9\gamma\gamma'} - 1\right)(\gamma - \gamma')$	1
	$\omega_{6,7}^+$	$\frac{V-\sqrt{16J^2+V^2}}{2}$	2
	$\omega_{8,9}^+$	0	2
	ω_{10}^+	$-\omega_1^+(J, -V) = \frac{V}{3} - \frac{48J^2+V^2}{9\gamma\gamma'} - \gamma'$	1

$$\gamma(J, V) = \left(\sqrt{\left(\frac{4J^2V}{3} - \frac{V^3}{27}\right)^2 - \left(\frac{16J^2}{3} + \frac{V^2}{9}\right)^3} - \frac{4J^2V}{3} + \frac{V^3}{27} \right)^{\frac{1}{3}} \quad \gamma' = \gamma(J, -V)$$

FIG. 7: Eigenvalues of H_+ with relative multiplicity (degeneracy), ordered by decreasing energy.

from H_+ to H_- , while the projections of states like $|1, 2\rangle_s$ do change all their signs. This is the reason why superpositions of (translationally) equivalent number eigenstates, like $|\Psi_B\rangle = |1, 3\rangle_s + |2, 4\rangle_s$, have the same correlations and entanglement independently from the sign of V , while superpositions of non-equivalent number eigenstates, like $|\Xi_B\rangle = |1, 4\rangle_s + |2, 4\rangle_s$, have a different evolution of their correlations under H_+ and H_- , as it was shown in Ref. [28]. Indeed, the change of sign in V introduces a relative phase between the components of the two number eigenstates, which is different for H_+ and H_- , thus leading to different evolutions of the states.

As an example, we have

$$U(t) (|1, 3\rangle_s + |2, 4\rangle_s) = \begin{cases} \sum_i (C_{1,3,i}^+ + C_{2,4,i}^+) |\Phi_i^+(t)\rangle & V > 0, \\ \sum_i (C_{1,3,i}^+ + C_{2,4,i}^+) |\Phi_i^-(t)\rangle & V < 0, \end{cases} \quad (19)$$

$$U(t) (|1, 4\rangle_s + |2, 4\rangle_s) = \begin{cases} \sum_i (C_{1,4,i}^+ + C_{2,4,i}^+) |\Phi_i^+(t)\rangle & V > 0, \\ \sum_i (-C_{1,4,i}^+ + C_{2,4,i}^+) |\Phi_i^-(t)\rangle & V < 0, \end{cases} \quad (20)$$

It should be emphasized that the coefficients $C_{j,k,i}^\pm$ changes sign when we change the sign of V , therefore we cannot observe this effect directly when we study a single number eigenstate (e.g., by setting $|\Psi(0)\rangle = |1, 3\rangle_s$), because the squared modulus of the projections do not depend on $\text{sgn}(C_{j,k,i}^\pm)$. Only superpositions of number eigenstates keep trace of the sign of the interaction [14, 27]. This is perhaps the reason why many previous works in the literature did not observe this dependence. Indeed, going back to our calculations on the 1D chain with $N = 30$, we notice that states like $|\Psi_1\rangle$ and $|\Psi_2\rangle$ are of the same kind, i.e. second nearest-neighbours like $|i, i+2\rangle_s$ (this is the reason why they show the same evolution of two-site correlations - except for a rigid translation), while the state $|\Psi_3\rangle$ is a third nearest-neighbour state, like $|i, i+3\rangle_s$. This is the reason why $|\Psi_1\rangle$ and $|\Psi_2\rangle$ have equal projections on the eigenstates of H_\pm , whereas the projections of $|\Psi_3\rangle$ are different. Therefore,

the linear combination of $|\Psi_1\rangle$ and $|\Psi_2\rangle$ is invariant under the exchange of $\text{sgn}(V)$, while the linear combination of $|\Psi_2\rangle$ and $|\Psi_3\rangle$ is not (some projections exchange sign for a state but not for the other).

Concerning the behaviour of a state like $|\Psi_6\rangle$, the effect of switching the sign of V is more visible at low potential energy, since for $V \sim J$ the main subband and the miniband are strongly mixed, such that each number eigenstate has a projection over all the eigenvectors of H_\pm , and states with different nature have therefore very different superpositions under H_+ and H_- . On the contrary, for large values of V/J the entanglement is not so much different, due to the strong separation between the subband and the miniband (see Fig. 6). Indeed, this separation implies that the projections of the bound state $|14, 14\rangle_s$ are almost completely contained in the miniband, while the ones of the scattering state $|14, 17\rangle_s$ are mainly in the main subband. Therefore, the expressions $C_{14,14,i}^\pm + C_{14,17,i}^\pm$ do not change significantly their (absolute) values when switching from H_+ to H_- since, for each i , only one coefficient in the sum is significantly different from zero.

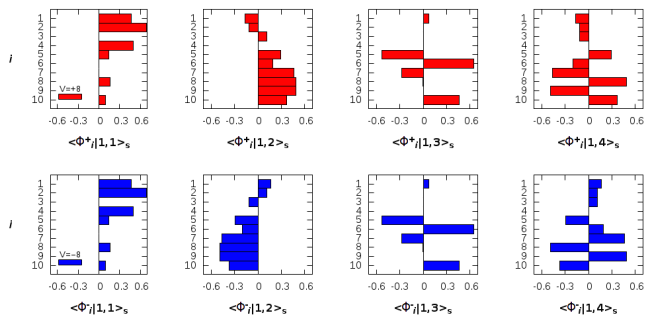


FIG. 8: Projections of number states $|1, 1\rangle_s$, $|1, 2\rangle_s$, $|1, 3\rangle_s$ and $|1, 4\rangle_s$ over the eigenstates of H_+ (first row, red) and H_- (second row, blue) for a potential energy of $|V| = 8$. Notice that, as expected, $|1, 4\rangle_s$ behaves like $|1, 2\rangle_s$, and their projections are also identical in modulus (since the two states are translationally equivalent).

This phenomenon may be better illustrated upon introducing a quantity $\Delta(V)$ that quantifies the difference between the projections of a state $|\Psi\rangle$ over the eigenstates of H_+ and H_- as a function of V . To this aim we first consider the sum the squared modulus of all the projections over the eigenstates with degenerate energies, i.e. $P^\pm(\omega) = \sum_{\omega_i=\omega} |\langle \Phi_i^\pm | \Psi \rangle|^2$. Then, for each projection $P(\omega)$ on a degenerate energy subspace, we evaluate the absolute difference between P at positive and negative V :

$$\Delta_\omega(V) = |P^+(\omega) - P^-(\omega)|^2, \quad (21)$$

in order to determine how much the projections of $|\Psi\rangle$ changes when switching from $|\Phi_i^+\rangle$ to $|\Phi_i^-\rangle$. Finally, we sum over the different energies of the Hamiltonian, and

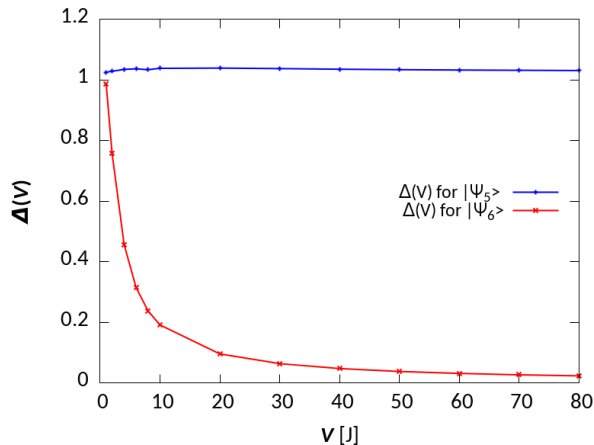


FIG. 9: Total difference $\Delta(V)$ among the projections of a state $|\Psi\rangle$ over the eigenstates of H for positive and negative V .

we get the desired figure of merit:

$$\Delta(V) = \sum_{\omega} \Delta_{\omega}(V). \quad (22)$$

As we can observe in Fig. 9, the quantity $\Delta(V)$ goes to zero for the state $|\Psi_6\rangle$, due to the progressive separation between the scattering subband and the miniband at increasing values of V/J . In turn, this is the reason for which the changes in entanglement and in correlations (when switching from positive to negative potentials) are more relevant at low interaction energies. A similar line of reasoning does not hold for $|\Psi_5\rangle$, which is composed by the scattering states $|14, 16\rangle_s$ and $|14, 17\rangle_s$, both belonging to the main subband: as we can see from Fig. 9, the differences in the projections $\Delta(V)$ for $|\Psi_5\rangle$ are nearly constant when we increase V . Indeed, we do not observe a significant change either in entanglement or in the correlation maps at increasing V , as we see in Figs. 4 and 5.

VI. CONCLUSIONS

In this paper, we have shown that in the dynamics of two identical bosons evolving according to the Hubbard Hamiltonian both two-site correlations and entanglement of particles are differently affected by the sign of the on-site interaction. These differences are more significant for low values of the interaction V , i.e. of the magnitude of the hopping amplitude J , thus making this regime achievable using current technologies [21, 22]. This behaviour arises from the fact that the projections of some localised number states on the eigenfunctions of the Hubbard model may change sign when we change the sign of V . Therefore, the effect of $\text{sgn}(V)$ may be observed in the evolution of linear superposition of number states. This also explains why these features have not been pointed

out and observed before, since most of the past literature was mainly focused on the study of single number states.

The quantitative dependence of correlations on the sign of V may be relevant, up to a factor 2 for entanglement. This phenomenon also provides a further degree of freedom for manipulating the correlations in a quantum walk, and may be exploited to perform specific tasks in quantum information processing.

Besides revealing novel features of the Hubbard model, and providing a probing technique for the sign of interaction, our results pave the way to further research, e.g. aimed at investigating whether this behaviour may be observed in some extensions of the Hubbard model - e.g. the Fermi-Hubbard model for spinless fermions (the so-called fermion-polaron model [73]) - or if it is an exclusive feature of bosonic Hubbard models. Indeed, some recent works [78] have shown a breaking of the symmetry $\pm V$ for long-range hopping in hard-core bosons. Besides, it seems worth to explore the signatures of long-range hopping and interactions (i.e., extended to first- and second-nearest neighbouring sites) on the dynamics and the entanglement of both bosonic and fermionic particles.

Acknowledgments

This work has been supported by UniMORE through FAR2014 and by EU through the collaborative H2020 project QuProCS (Grant Agreement 641277). The authors thank Ilaria Siloi for fruitful discussions. PB and MGAP are members of INdAM.

Appendix A: Invariance under Boost and Time-reversal transformations

In this section we want to further discuss the symmetries of the Hamiltonians $H_{\pm} = H_N(J, \pm V)$ [14, 27] in order to better appreciate the results presented in the body of the paper. In particular, we want to emphasise that the expectation value of an operator O on state $|\psi(t)\rangle_{\pm} = \exp(-iH_{\pm}t)|\psi_0\rangle$ is independent from the sign of V if both the initial state $|\psi_0\rangle$ and O are invariant under both *boost transformation* and *time reversal transformation*. In order to better illustrate this features we will go through the explicit proof of the invariance.

The idempotent Hermitian *boost operator*, $B = B^{\dagger}$, $B^2 = 1$, is defined by its action in k space: $Ba_k^{\dagger}B = a_{k+\pi}^{\dagger}$, whereas in the x space we have $Bc_jB = e^{-i\pi j}c_j$. As a consequence, we may write

$$BH_{\pm}B = -H_{\mp}. \quad (A1)$$

Being B a unitary operator any eigenstate of B is actually invariant under the action of B . The same discussion does not hold, of course, for combinations of eigenstates belonging to different eigenvalues. The *time reversal operator* is the antiunitary operator Θ defined by

$\Theta e^{-iH_{\pm}t}\Theta^{\dagger} = e^{+iH_{\pm}t}$ and $\Theta|\psi_0\rangle = |\psi_0^*\rangle$ and which may be written as $\Theta = KU$, where U is a unitary operator and K is the complex-conjugation operator. An operator is said to have a well defined symmetry under time reversal if it is even (invariant) or odd, $\Theta O\Theta^{\dagger} = \pm O$.

Let us consider now the expectation value of O under H_+ , i.e. $\langle O(t) \rangle_+ = \langle \psi_0 | \exp(+iH_+t) O \exp(-iH_+t) | \psi_0 \rangle$. Under the hypothesis that both O and $|\psi_0\rangle$ are invariant under B we have

$$\begin{aligned} \langle O(t) \rangle_+ &= \langle \psi_0 | \exp(-iH_-t) O \exp(+iH_-t) | \psi_0 \rangle \\ &= \langle O(-t) \rangle_- . \end{aligned} \quad (\text{A2})$$

If we also consider the invariance under time reversal of both O and $|\psi_0\rangle$, we get finally

$$\begin{aligned} \langle O(t) \rangle_+ &= \langle O(-t) \rangle_- \\ &= \langle \psi_0 | \exp(+iH_-t) O \exp(-iH_-t) | \psi_0 \rangle \\ &= \langle O(t) \rangle_- , \end{aligned} \quad (\text{A3})$$

so that the switching of the sign of the potential produces no effect on the expectation value of O . Overall,

we may conclude that in general, if the state and the observable are invariant under boost transformation, when we switch the sign of the potential V we actually reverse the direction of time: some observables, like the entanglement, are not affected by this operations, while others do. In particular, if we look at the correlation maps, changing the direction of time is equal to changing sign to all the velocity components of the wave-functions, so that left and right directions are reversed (i.e., the correlation maps become specular). However, this phenomenon is not observable if the velocity composition is symmetrical (i.e., it determines a symmetrical expansion on the map), but in the opposite case it can be spotted. This is particularly apparent for states like $|\psi\rangle = |14, 16\rangle_s + |15, 17\rangle_s$, where entanglement and correlation maps are identical (both states have the same eigenvalue with respect to B). On the other hand, if we add a complex relative phase, i.e. $|\psi\rangle = |14, 16\rangle_s + i|15, 17\rangle_s$, we break the time-reversal invariance and we make the velocity composition asymmetrical. In this case, the entanglement does not change its dynamics, but the correlation maps are reversed with respect to their anti-diagonal.

-
- [1] F. H. Essler, H. Frahm, F. Göhmann, A. Klümper, and V. E. Korepin, *The one-dimensional Hubbard model* (Cambridge University Press, 2005).
- [2] A. Montorsi, *The Hubbard Model: A Reprint Volume* (World Scientific, 1992).
- [3] E. H. Lieb and F. Wu, *Physica A* **321**, 1 (2003).
- [4] L. Amico, R. Fazio, A. Osterloh, and V. Vedral, *Rev. Mod. Phys.* **80**, 517 (2008).
- [5] P. M. Preiss, R. Ma, M. E. Tai, A. Lukin, M. Rispoli, P. Zupancic, Y. Lahini, R. Islam, and M. Greiner, *Science* **347**, 1229 (2015).
- [6] L.-M. Duan, E. Demler, and M. D. Lukin, *Phys. Rev. Lett.* **91**, 090402 (2003).
- [7] T. Fukuhara, P. Schauß, M. Endres, S. Hild, M. Cheneau, I. Bloch, and C. Gross, *Nature* **502**, 76 (2013).
- [8] D. Jaksch and P. Zoller, *Ann. Phys.* **315**, 52 (2005), special Issue.
- [9] T. Fukuhara, A. Kantian, M. Endres, M. Cheneau, P. Schauß, S. Hild, D. Bellem, U. Schollwöck, T. Giamarchi, C. Gross, et al., *Nature Phys.* **9**, 235 (2013).
- [10] H. J. Schulz, *Phys. Rev. Lett.* **64**, 2831 (1990).
- [11] Y. Lahini, M. Verbin, S. D. Huber, Y. Bromberg, R. Pughatch, and Y. Silberberg, *Phys. Rev. A* **86**, 011603 (2012).
- [12] Y. Bromberg, Y. Lahini, E. Small, and Y. Silberberg, *Nature Phot.* **4**, 721 (2010).
- [13] F. Lederer, G. I. Stegeman, D. N. Christodoulides, G. Asanto, M. Segev, and Y. Silberberg, *Physics Reports* **463**, 1 (2008).
- [14] C. Lee, A. Rai, C. Noh, and D. G. Angelakis, *Phys. Rev. A* **89**, 023823 (2014).
- [15] S. Longhi, *J. Phys. B* **44**, 051001 (2011).
- [16] T. Matsubara and H. Matsuda, *Progr. Theor. Phys.* **16**, 569 (1956).
- [17] X. Qin, Y. Ke, X. Guan, Z. Li, N. Andrei, and C. Lee, *Phys. Rev. A* **90**, 062301 (2014).
- [18] L. Wang, L. Wang, and Y. Zhang, *Phys. Rev. A* **90**, 063618 (2014).
- [19] L. Wang, N. Liu, S. Chen, and Y. Zhang, *Phys. Rev. A* **92**, 053606 (2015).
- [20] J. Hecker Denschlag and A. J. Daley, in *Proceedings of the International School of Physics "Enrico Fermi"* (IOS Press Ebooks, 2007), vol. 164.
- [21] K. Winkler, G. Thalhammer, F. Lang, R. Grimm, J. H. Denschlag, A. Daley, A. Kantian, H. Büchler, and P. Zoller, *Nature* **441**, 853 (2006).
- [22] L. Wang, Y. Hao, and S. Chen, *Phys. Rev. A* **81**, 063637 (2010).
- [23] S. Fölling, S. Trotzky, P. Cheinet, M. Feld, R. Saers, A. Widera, T. Müller, and I. Bloch, *Nature* **448**, 1029 (2007).
- [24] R. Piil and K. Mølmer, *Phys. Rev. A* **76**, 023607 (2007).
- [25] L. Wang, Y. Hao, and S. Chen, *Eur. Phys. J. D* **48**, 229 (2008).
- [26] M. Valiente and D. Petrosyan, *J. Phys. B* **41**, 161002 (2008).
- [27] U. Schneider, L. Hackermüller, J. P. Ronzheimer, S. Will, S. Braun, T. Best, I. Bloch, E. Demler, S. Mandt, D. Rasch, et al., *Nature Phys.* **8**, 213 (2012).
- [28] A. Beggi, F. Buscemi, and P. Bordone, *Quantum Inf. Proc.* **15**, 3711 (2016).
- [29] C. Benedetti, F. Buscemi, P. Bordone, and M. G. A. Paris, *Phys. Rev. A* **89**, 032114 (2014).
- [30] M. G. A. Paris, *Physica A* **413**, 256 (2014).
- [31] D. Tamascelli, C. Benedetti, S. Olivares, and M. G. A. Paris, *Phys. Rev. A* **94**, 042129 (2016).
- [32] I. Siloi, C. Benedetti, E. Piccinini, J. Piilo, S. Maniscalco, M. G. A. Paris, and P. Bordone, *Phys. Rev. A* **95**, 022106 (2017).
- [33] J. Kempe, *Contemp. Phys.* **44**, 307 (2003).

- [34] S. Venegas-Andraca, *Quantum Inf. Proc.* **11**, 1015 (2012).
- [35] A. Ambainis, *Int. J. Quantum Inf.* **01**, 507 (2003).
- [36] R. Portugal, *Quantum walks and search algorithms* (Springer Science & Business Media, 2013).
- [37] S. E. Venegas-Andraca, *Synthesis Lectures on Quantum Computing* **1**, 1 (2008).
- [38] D. Tamascelli and L. Zanetti, *J.Phys. A* **47**, 325302 (2014).
- [39] Y. Bromberg, Y. Lahini, R. Morandotti, and Y. Silberberg, *Phys. Rev. Lett.* **102**, 253904 (2009).
- [40] A. Peruzzo, M. Lobino, J. C. F. Matthews, N. Matsuda, A. Politi, K. Poulios, X.-Q. Zhou, Y. Lahini, N. Ismail, K. Wrohoff, et al., *Science* **329**, 1500 (2010).
- [41] A. Rai, G. S. Agarwal, and J. H. H. Perk, *Phys. Rev. A* **78**, 042304 (2008).
- [42] D. Tamascelli, S. Olivares, S. Rossotti, R. Osellame, and M. G. A. Paris, *Phys. Rev. Lett.* **116**, 26054 (2016).
- [43] J. Wang and K. Manouchehri, *Physical implementation of quantum walks* (Springer, 2013).
- [44] M. A. Broome, A. Fedrizzi, S. Rahimi-Keshari, J. Dove, S. Aaronson, T. C. Ralph, and A. G. White, *Science* **339**, 794 (2013).
- [45] J. B. Spring, B. J. Metcalf, P. C. Humphreys, W. S. Kolthammer, X.-M. Jin, M. Barbieri, A. Datta, N. Thomas-Peter, N. K. Langford, D. Kundys, et al., *Science* **339**, 798 (2013).
- [46] M. Tillmann, B. Dakić, R. Heilmann, S. Nolte, A. Szameit, and P. Walther, *Nature Phot.* **7**, 540 (2013).
- [47] J. D. Franson, *Science* **339**, 767 (2013).
- [48] C. Benedetti, F. Buscemi, and P. Bordone, *Phys. Rev. A* **85**, 042314 (2012).
- [49] K. Mayer, M. C. Tichy, F. Mintert, T. Konrad, and A. Buchleitner, *Phys. Rev. A* **83**, 062307 (2011).
- [50] J. Schliemann, J. I. Cirac, M. Kuś, M. Lewenstein, and D. Loss, *Phys. Rev. A* **64**, 022303 (2001).
- [51] K. Eckert, J. Schliemann, D. Bru, and M. Lewenstein, *Ann. Phys.* **299**, 88 (2002).
- [52] F. Buscemi, P. Bordone, and A. Bertoni, *Phys. Rev. A* **73**, 052312 (2006).
- [53] F. Buscemi, P. Bordone, and A. Bertoni, *Phys. Rev. A* **75**, 032301 (2007).
- [54] P. Zanardi, *Phys. Rev. A* **65**, 042101 (2002).
- [55] G. C. Ghirardi, L. Marinatto, and T. Weber, *J. Stat. Phys.* **108**, 49 (2002).
- [56] G. C. Ghirardi and L. Marinatto, *Phys. Rev. A* **70**, 012109 (2004).
- [57] F. Benatti, R. Floreanini, and K. Titimbo, *Open Sys. Inf. Dyn.* **21**, 1440003 (2014).
- [58] H. M. Wiseman and J. A. Vaccaro, *Phys. Rev. Lett.* **91**, 097902 (2003).
- [59] M. R. Dowling, A. C. Doherty, and H. M. Wiseman, *Phys. Rev. A* **73**, 052323 (2006).
- [60] T. Sasaki, T. Ichikawa, and I. Tsutsui, *Phys. Rev. A* **83**, 012113 (2011).
- [61] F. Iemini, T. Maciel, T. Debarba, and R. Vianna, *Quantum Inf. Proc.* **12**, 733 (2013).
- [62] F. Iemini and R. O. Vianna, *Phys. Rev. A* **87**, 022327 (2013).
- [63] F. Iemini, T. Debarba, and R. O. Vianna, *Phys. Rev. A* **89**, 032324 (2014).
- [64] A. Reusch, J. Sperling, and W. Vogel, *Phys. Rev. A* **91**, 042324 (2015).
- [65] P. Zanardi, D. A. Lidar, and S. Lloyd, *Phys. Rev. Lett.* **92**, 060402 (2004).
- [66] H. Barnum, E. Knill, G. Ortiz, R. Somma, and L. Viola, *Phys. Rev. Lett.* **92**, 107902 (2004).
- [67] F. Benatti, R. Floreanini, and U. Marzolino, *Phys. Rev. A* **85**, 042329 (2012).
- [68] F. Benatti, R. Floreanini, and U. Marzolino, *Phys. Rev. A* **89**, 032326 (2014).
- [69] L. Mazza, D. Rossini, R. Fazio, and M. Endres, *New J. Phys.* **17**, 013015 (2015).
- [70] F. Iemini, T. O. Maciel, and R. O. Vianna, *Phys. Rev. B* **92**, 075423 (2015).
- [71] F. Buscemi and P. Bordone, *Phys. Rev. A* **84**, 022303 (2011).
- [72] D. de Falco and D. Tamascelli, *J. Phys. A* **39**, 5873 (2006).
- [73] A. Scott, J. Eilbeck, and H. Gilhøj, *Physica D* **78**, 194 (1994).
- [74] M. Valiente, *Phys. Rev. A* **81**, 042102 (2010).
- [75] D. Girolami and G. Adesso, *Phys. Rev. A* **84**, 052110 (2011).
- [76] S. Lee, D. P. Chi, S. D. Oh, and J. Kim, *Phys. Rev. A* **68**, 062304 (2003).
- [77] E. Piccinini, C. Benedetti, I. Siloi, M. G. A. Paris, and P. Bordone, *Comp. Phys. Comm.* **215**, 235 (2017).
- [78] T. Chattaraj and R. V. Kreams, *Phys. Rev. A* **94**, 023601 (2016).